Modeling and Simulation of Tool Induced Soil Resistance with Application to Excavator Machines

Heng Liu

Thesis submitted to
the Faculty of Graduate Studies
in partial fulfilment of
the requirements for the degree of
Master of Science

Department of Engineering
Faculty of Mechanical
University of Manitoba
Winnipeg, Manitoba

2016

Abstract

To evaluate and test control systems designed for heavy duty hydraulic excavator, it is important to simulate the force acting on the bucket during its excavation process. The study of soil-tool interaction contributes to the prediction and simulation of resistive forces experienced at the tool during digging. Even though many different finite element (FE) models have been developed in the past to study soil-tool interaction process, there is still needs to study the effects of soil-tool friction coefficient. The main objective of this thesis is to utilize finite element model to simulate the soil-tool interaction process, with the focus on the application of excavation, to study the effects of soil-tool friction coefficient on soil failure zone, soil resistive force, and stress distribution on the cutting tool by utilizing finite element model to simulate the soil-tool interaction process.

In this thesis, 2D finite element (FE) model is built with different rake angles ranging from 30˚ to 90˚ and soil-tool friction coefficients ranging from 0 to 0.424 with two different soil types: clayey soil and sandy loam soil. Non-associate Drucker-Prager constitutive law is applied to govern soil's stress-strain relationship. Contact elements are attached to the contacting surface of blade and soil to simulate their contact phenomena. By using plastic strain intensity, the soil failure zone of each FE model is identified. Soil failure angle obtained from the FE model is compared with results obtained from three previously used soil failure angle analytical models. As the predicted soil resistive force by the analytical method is directly related to the accuracy of the proposed failure zone, the soil failure zone analytical model that has the best accordance with the FE model is recommended for future use. Stress distribution on the tool surface is studied for all rake angles and soil-tool friction coefficients. All analytical models assume the soil resistive force acts on the tool tip (the bottom edge of the tool), the results of this study shows how the stress is distributed across the cutting tool with different rake angles and soil-tool friction coefficients and the research also shows how to add an equivalent moment to the bottom edge of

the tool to compensate the actual stress distribution. Validation of the FE models are examined from two aspects: soil failure plane and soil displacement field. Eventually, it is proposed to use the obtained knowledge from FE model in simulating resistive force during a typical digging cycle.

Acknowledgments

I would like to thank my advisor, Dr. Nariman Sepehri, for his guidance and collaboration throughout my program.

I also want to acknowledge the enormous support received from my committee members Dr. Ying Chen and Dr. Nan Wu.

I am grateful to the support of my family for their encouragement and advice throughout my program.

Table of Contents

List of Tables

List of Figures

List of Symbols

P	Total cutting force on blade
γ	Soil unit weight
d	Cutting depth of cutting blade
c	Soil cohesion
N_γ	Factor depend on soil internal angle of friction
N_c	Factor depend on soil geometry
N_q	Factor depend on soil-tool friction
q	Surcharge pressure vertically acting on the soil surface
w	Tool Width
ρ	Tool rake angle
β	Soil failure angle
δ	Soil-tool friction angle
$\emptyset$	Soil internal friction angle
W	Weight of soil wedge
L_t	Length of the tool
L_f	Length of the failure surface
Q	Weight of the surcharge
Ca	Adhesion between the soil and tool
R	Force of the soil resisting the moving of the wedge
s	Shear strength of soil
σ_n	Pressure acting perpendicularly on the shearing surface
F_C	Friction force
μ	Friction coefficient
F_N	Force acting perpendicular on the interfacing surfaces
f	Yield surface of Drucker-Prager yield criterion
J_1	First invariant of the stress tensor
J_{2D}	Second invariant of deviatoric stress tensor
α	Material parameter
k	Material parameter

Chapter 1 Introduction

1.1 Background of the Problem

The study of soil-tool interaction forces involved in the earthmoving procedure can be dated back to five decades ago. This field of study is important because energy supplied during the earthmoving procedure is mainly consumed during soil-tool interaction. A better understanding of soil-tool interaction not only can be used to optimize tool design to improve energy efficiency but also can be applied to other areas such as real time simulator and control system evaluation. [1] [2] [3]

In the past studies, many models have been proposed to describe soil-tool interactions. These models can be categorized into three main groups: analytical models, empirical models and numerical models.

Analytical models are developed based on predefined soil failure zone and simplified static equilibrium analysis. The resulting models have limited abilities to describe the soil-tool interaction phenomena. [4] The presumed soil failure zone has significant influence on the force prediction and should be studied before the analytical method is applied. Nevertheless, this approach is widely used as it has high flexibility, has clear representation of forces involved, and is very easy to be utilized.

Empirical models have moderately accurate prediction on soil cutting force. But this approach requires extensive experiments and usually has high cost. Also as the obtained model does not express forces in common parameters of soil, it can be difficult to extend its use to different regions.

Numerical models have been used to understand the reality of soil-tool interaction phenomenon in the past studies. Information of soil failure zone, soil displacement field, and stress distribution on the cutting tool can be obtained from this ap-

proach. With all the advantages of this approach to model soil-tool interaction, numerical models are not suitable for real time implementation due to its computational expense. [5]

As no approach is superior amongst the others, it would beneficial to use FE model to learn knowledge of soil-tool interaction and then apply this knowledge to analytical model for real time simulation. Even though many Fe models have been developed in the past to study the soil-tool interaction, there are not enough research conducted in studying the effects of soil-tool friction coefficient on soil failure zone, soil resistive force and stress distribution on the tool.

1.2 Objectives and Scope of the Research

Although many different FE models have been developed in the past to study soil-tool interaction pheromones, there are not enough researches conducted in studying the effects of soil-tool friction coefficient on soil failure zone, soil resistive force, and stress distribution on the tool.

This research aims to contribute to the development of current knowledge of earthmoving process by thoroughly investigate the effects of soil-tool contact property on their contact phenomenon, soil failure zone, and force distribution on cutting tool during the earthmoving process with FE model. This thesis also demonstrates how to apply the obtained knowledge from FE model to generate resistive force in the application of hydraulic excavator.

The specific objectives to achieve this main goal are identified as follows:

- Firstly the research will utilize FE model to investigate effects of soil-tool friction coefficient on soil failure zone, soil resistive force, and stress distribution on cutting blade.
- Secondly knowledge obtained from FE model will be applied to simulate resistive force of soil during a typical digging process

1.3 Research Methodology

Three different approaches that are conventionally used to simulate and predict soil resistive force are reviewed. These approaches are analytical approach, empirical approach, and numerical approach. Pros and cons of each approach are discussed.

FE model with different rake angles, friction coefficients, and soil types are built to study the interaction between blade and soil. Soil failure zones are measured for each model. Effect of meshing density is studied using FE models with rake angle of 50˚ and soil-tool friction coefficient of 0. Soil failure angles obtained from FE models are compared to the results obtained from three different analytical formulas that have been used in previous studies. Stress distribution on the cutting blade is studied. Location of the equivalent point force on the blade is established.

Kinematic study is used to obtain the trajectory of a digging bucket during a typical excavation process with the inputs of displacements of its three actuators. With the trajectory of the bottom blade of the bucket, analytical method is used to simulate soil resistive force acting on the blade during its digging action.

1.4 Thesis Structure

This thesis is organized into six chapters. Chapter 1 is the introduction section. Chapter 2 covers a comprehensive review on the approaches that are used to study the tool-induced soil resistances. Advantages and limitations of each approach are discussed. Soil properties and parameters that are used in the analytical models and numerical models are reviewed. Additionally, constitutive models that have been used with finite element models are also discussed. Chapter 3 covers the numerical modeling of the soil blade interaction. Chapter 4 discusses detailed results obtained from extensive numerical models. Validation of models is also covered in this chapter. The results obtained from numerical models are then applied to simulate digging resistive force in a typical excavation process. The process of simulating digging resistive force during a typical excavation process is presented in Chapter 5. Chapter 6

presents conclusions of the research and recommendations for future work as extension of current study.

Chapter 2 Background of Tool Induced Soil Resistance Model

2.1 Introduction

Earthmoving procedure transfers soil from its original location, therefore involves breaking and loosening of soil. The resistance force induced by earthmoving tools mainly depends on the tool geometry and soil properties. Although earthmoving tools are very different in shapes and functions, they can be generally grouped into three categories: blade, ripper and shovel. Examples of tools that fall into the blade category are bulldozer front and back blades, road graders, and hauling scrapers. These machines cut and push soil with straight-edged blades, cutting depth is usually less than the width of the blade. Tools that fall into the ripper category can often be found attached to graders and bulldozers. They are used to cut and loosen soil, pavement and soft rock layers. These tools are much narrower comparing to their cutting depth. Shovel types of tools consists of a bottom cutting plate with side plates, which will confine the soil or other materials that can be cut and lifted up in the horizontal direction. With shovels cut and pushing forward, a vertical-sided trench are usually formed. [6] [7]

The study of soil-tool interaction is primarily started by Terzaghi with his passive earth pressure theory. Since then different approaches have been proposed and developed to study the interaction between soil and tools naming: analytical model, empirical model, and numerical model. With each approach has its own advantages and disadvantages, no approach is superior amongst the others.

2.2 Analytical Soil Resistance Models

Based on Terzaghi's passive earth pressure theory, two- and three-dimensional analytical models are developed since then. Although these models may vary a lot in some aspects, they are all based on the same assumptions that soils are homogeneous, isotropic, semi-infinite, and ideal plastic; soil fails with a presumed failure zone. The failure profile of soil is usually considered to be a curved line. This curved line is approximated with a straight line, for the ease of calculation, in some of the analytical models. [6] [7]

Analytical resistance models, also called universal earthmoving equation models, assume that a certain failure shape develops during the earthmoving procedure. And by solving the static equilibrium equations with its corresponding boundary conditions, the minimal resisting force that is required to break the soils is obtained. These models usually are comprised of components of forces such as gravitational, cohesional, adhesional and frictional forces. Among all the force components, the cohesional force is the most significant and the adhesional force is almost negligible. [8]

2.2.1 Two-dimensional Analytical Model

Reece's model

As the mechanics of earthmoving are similar to the bearing capacity of shallow foundations on soil, based on Terzaghi's bearing capacity theory, Reece proposed the universal earthmoving equation with three major components:

$$P = \left(\gamma . d^2 . N_\gamma \ + \ c . d . N_c + q . \gamma . N_q\right) . w \tag{1}$$

where

$$N_\gamma = \frac{cot\rho + cot\beta}{2[\cos(\rho + \delta) + \sin(\rho + \delta) \, . \cot(\beta + \emptyset)]} \tag{2}$$

$$N_c = \frac{1 + cot\beta . \cot(\beta + \emptyset)}{[\cos(\rho + \delta) + \sin(\rho + \delta) \, . \cot(\beta + \emptyset)]} \tag{3}$$

$$N_q = \frac{cot\rho . \cot\beta}{[\cos(\rho+\delta)+\sin(\rho+\delta).\cot(\beta+\emptyset)]} \quad (4)$$

P is the total cutting force, γ is the soil unit weight, d is the cutting depth, c is the soil cohesion, q is the surcharge pressure vertically acting on the soil surface, w is tool width, and N_γ, N_c, N_q are factors depend on soil internal angle of friction, soil geometry, and friction angle between tool and soil.

Reece's model is suitable to be used for soil cutting tools with wide blades relative to their depths of operation. As shown in Figure 1, failure shape of soil is assumed to be a triangle. The failure angle (β) is defined as the angle between straight slip line and the terrain profile. By solving its static equilibrium, soil resistive force can then be calculated. [8] [9]

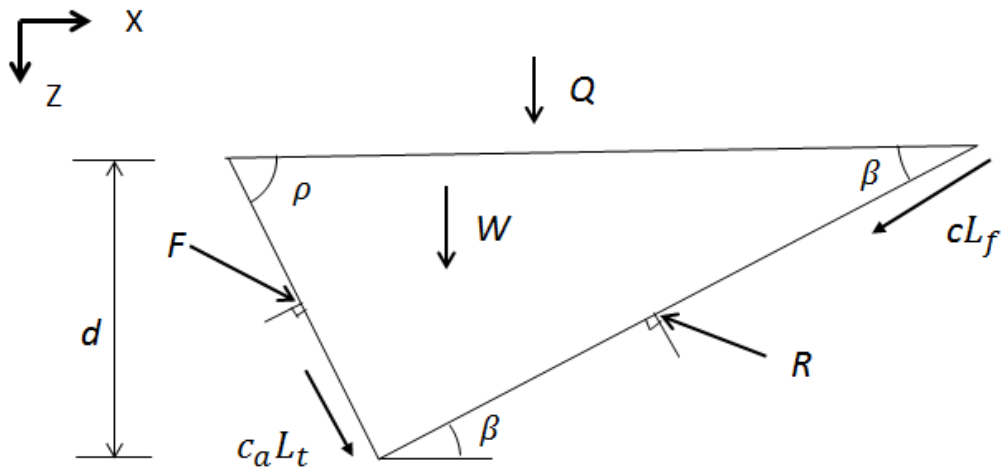

Figure 1 Static analysis of wedge model

W is the weight of wedge, Lt is the length of the tool, Lf is the length of the failure surface, Q is the weight of the surcharge, ∅ is the soil-soil friction angle, c is the cohesiveness of the soil, Ca is the adhesion between the soil and blade, $\delta$is the soil-tool friction angle, β is the failure surface angle, ρ is the rake angle, d is the

depth of the tool in the soil, R is the force of the soil resisting the moving of the wedge, and F is the force exerted by the tool on the wedge.

2.2.2 Three-dimensional Analytical Models

Two dimensional models are suitable to be used for cutting tools with wide blades relative to their depths of operation. To predict cutting force of tools that are used in other cases, three-dimensional analytical models are proposed by many researchers and are reviewed in this section.

Payne's model

Payne's model is the first three-dimensional soil failure model. This model only predicts the shape of the failure zone for narrow tillage tools, and no equations were developed to predict cutting forces. With observation of experiments, proposed failure zone consists of a triangular center wedge, a center crescent, and two side blocks as shown in Figure 2. [10]

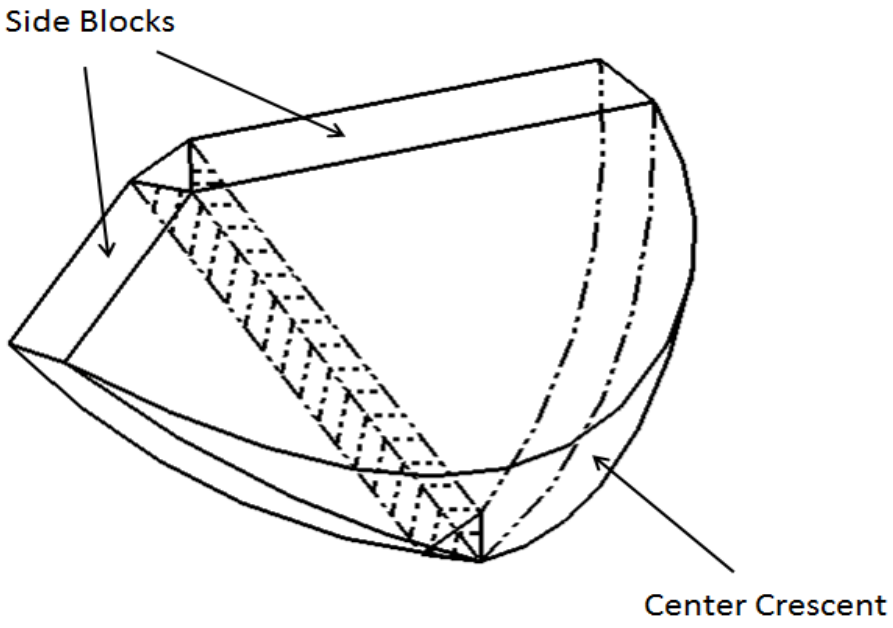

Figure 2 Payne's soil failure model

Hettiaratch-Reece model

This three-dimensional model developed by Hettiaratchi and Reece (1967) consists of a forward failure zone as a result of the forward movement of the tool and a horizontal transverse failure zone as a result of the movement of the soil pushed away from the center. Based on the failure zone assumption, the total resultant force on the cutting tool can be divided into two vector forces due to forward failure (P_f) and the sideways failure (P_s). Extensive experiments were conducted by Hettiaratchi and Reece (1967) to investigate the validity of the model. Experimental result shows that the model over-predicted the tool forces for tine at low depth-to-width ratios. [11]

Godwin-Spoor model

Two different models were proposed by Godwin and Spoor to predict draft forces for narrow tillage tines. The two models are to be used for tools operating at depths less of greater than critical depth repetitively. The model that is used for tool with proposed failure pattern has a parallel center wedge with two curved side crescents. The total force was determined as [12]

McKyes-Ali model

Mckyes and Ali (1977) proposed a three-dimensional model that has the similar failure zone to the Godwin-Spoor model, which was also composed of a center wedge and two side crescents. One of the major differences between the two models is that in McKyes-Ali model, rupture distance was determined by failure angle, tool penetration depth, and tool rake angle. Prior knowledge of rupture distance is not required, and hence easier to be used. [13]

2.3 Finite Element Models

With the development of computer's calculation ability and its increased accessibility, numerical models are used more and more to simulate the interaction between soil and earthmoving tools. Compared to other approaches, not only can finite element method investigate the total soil force acting on the tool, it also allows researchers to study the progressive failure zone, stress distribution on the tools, and

soil displacement field. In this way, this approach allows for a better understanding of the interaction between soil and tool, and is helpful in perfecting other simulation methods. The downside of this method is that it requires relative large amount of time for calculation, and thus it is not suitable for real time simulation.

The first finite element model to simulate soil-machine interaction was done by Yong and Hanna. They used the plane strain model to simulate interaction between wide blade and soil. The geometry and meshing of the model is shown in Figure 3. The body of soil is modeled with linear triangular elements and the interaction of soil-tool and soil-soil were modeled with 1D joint element. They assumed the soil is nonlinear elastic material. Their research provides detailed results on progression of soil failure zone, normal pressures developed at the blade, and stress distribution on the blade. [14]

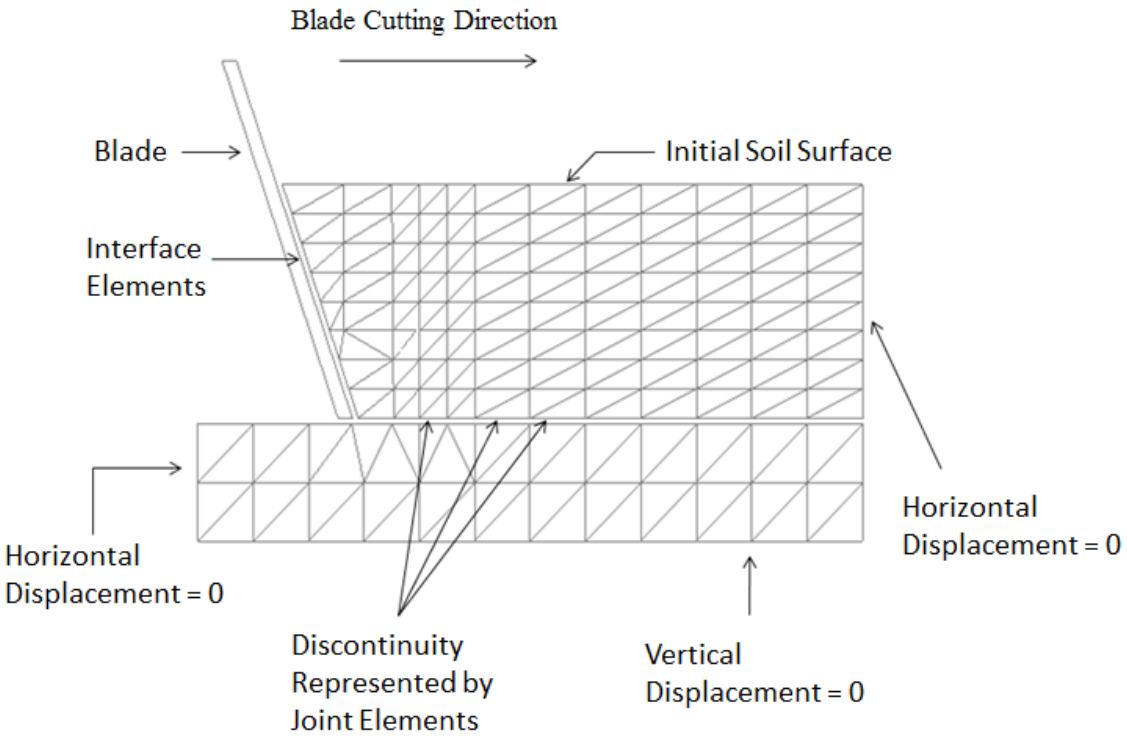

Figure 3 Geometry and meshing of Yong and Hanna's model

Chi and Kushwaha developed a nonlinear 3D finite element model to study the interaction of soil and a narrow tillage tool. Figure 4 shows the finite element mesh for soil. Tetrahedral constant strain elements were used in their model. As the model is symmetrical, only half of the total region was developed for the analysis. Hyperbolic constitutive model proposed by Duncan and Chang was used to govern the stress strain relationship of soil. Friction at the soil-tool interface was taken into account. They modeled a progressive and continuous cutting process. In their research, they used the maximum draft force obtained during the soil cutting as the failure point of soil wedge. That corresponding reaction force was taken as the required force for soil cutting. The results shows that the draft forces decreased as the rake angle decreased, but stayed constant for rake angles less than 45° [15]

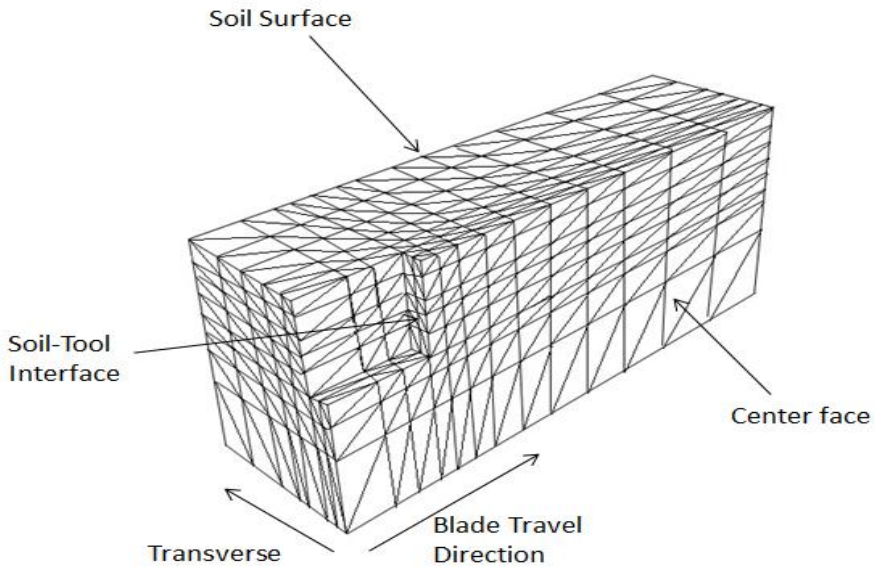

Figure 4 Meshing of Chi and Kushwaha's model

A dynamic soil-blade interaction model was developed by Shen and Kushwaha to investigate soil cutting process. A 2D plane strain model was used to predict the draft force of a vertical blade. Duncan and Chang's hyperbolic model was used for soil constitutive relation and soil failure was based on the Mohr-Coulomb criterion. In their research, results obtained from soil bin tests and modeling are compared. The comparison showed that the results obtained from two methods are very close.

For speed less than 9km/h during the soil cutting process, blade draft force increased with the increase of blade's speed. And for speed higher than 9km/h, draft force increased up to a peak value and slowly dropped as the displacement of blade increase. [16]

Mouazen and Nemenyi proposed a 3D finite element model to study the interaction between subsoiler and soil. In their model properties of a non-homogeneous sandy loam soil was used. The soil was modeled with 8-node brick elements. Associated Drucker-Prager constitutive law was used to govern the soil's stress-strain relationship. They studied the subsoiler in four different geometry conditions: vertical shank with 31° inclined chisel, vertical shank with 23° inclined chisel, vertical shank with 15° inclined chisel, and 75° rake angle shank with 15° inclined chisel. Adhesion between dry soil and tool was neglected in their model and Coulomb friction model was used to describe interaction between soil and tool. Results obtained from lab soil bin test are used to verify their simulated results. It is shown that the finite element model over predict the results obtained for both homogeneous and non-homogeneous soil. The over-prediction ranged from 11% to 16.8% for non-homogeneous soils and 15% to 18.4% for the homogenous soil. [17]

A 3D FE dynamic model to simulate soil-blade interaction was proposed by Abo-Elnor and Hamilton. [18] A 3D 8-noded brick element was used to model both sandy soil and the blade. Mesh density was found to have a significant effect on the predicted results. It is found that with the increase of the mesh density the predicted force decreases.

Rosa and Wolfsohn used hypoelastic soil constitutive relationship and a nonlinear Young's modulus to study high speed tillage process. Strain effect is considered in their model. Narrow cutting tools with two different shapes were used in their model. One tool is a flat blade while the other has a triangular edge. Experiments were conducted with forward speed between 0.5 to 10 m/s over a distance of 1 to 3 m. Their model overpredicts 1% at 2.8m/s and 25% at 8.4 m/s for the tool with triangular edge. It is concluded that the soil model is not satisfactory in predating the soil resistive force. [19]

2.4 Soil Properties and Key Parameters

Laboratory testing, such as unconfined uniaxial and axisymmetric compression tests, with a soil sample is a conventional practice for determining the engineering properties of a soil. These engineering properties are essential for the constitutive models and analytical models that are used in soil engineering. To be able to model and simulate interaction between soil and earthmoving tools with numerical models and analytical models, the necessary parameters can be separated into four categories:

- Tool parameters: tool penetration depth (d), tool rake angle (α), and width of tool(w)
- Soil parameters: soil density (γ), soil cohesion (C), soil failure angle (ρ), soil internal friction angle ($\emptyset$), Young's modulus of elasticity(E), and Poisson's ratio (v).
- Soil-tool interface parameters: soil-tool friction angle (δ)
- Surcharge condition: terrain profile

2.4.1 Soil Parameters and Mechanics

Soil is a mixture of sediments which may contains gravel, sand, silt and clay. The consistency of soil is determined by water content and mixture ratio. [20]

Soil density is usually expressed as its weight per unit volume. Some of the typical natural soils have unit weight ranging from 16 kN/m^3 to 22 kN/m^3. Sands generally have relative high densities while clays generally have relative low densities. [21]

Among the various types of failure, shear failure is concerned in the soil failure problem. In order to describe the soil strength and soil failure mechanism, Coulomb proposed that the shear strength of soil is determined by soil internal friction and cohesion. Their relationship is shown as follow:

$$s = c + \sigma_n tan\emptyset \quad (5)$$

As from the equation, cohesion (c) of soil contributes a constant value to shear strength (s) regardless of the normal pressure acting while the contribution of internal friction is proportional to the pressure (σ_n) acting perpendicularly on the shearing surface. [6] $tan\emptyset$ is the coefficient of internal friction and $\emptyset$ is also called soil internal friction angle ($\emptyset$). It can be directly obtained experimentally as the angle of repose of a pile of dry, uncompacted granular material. Soil internal friction angle can be influenced by many factors including soil particle shape, size, compaction condition and type of material. Compared to loose sand, compacted sand tends to have a higher friction angle. Typical friction angle of cohesionless granular soils ranges from 27 degree to 50 degree while typical friction angle of cohesive soils ranges from 10 degree to 30 degree. [22] Direct shear test and triaxial test are commonly used to obtain the shear strength parameters of various soil specimens in the laboratory. [23]

Soil dilatancy is the tendency of soils to change volume while shearing. Soil dilatancy angle can be obtained by conducting strain measurements in triaxial compression testing. Volume of soil increases if they are initially dense, and volume of soil decreases if they are initially loose. [24]

Soil failure angle is also called soil shear angle. There are three formulas that are commonly used to predict the shear angles of soil. They are used with analytical models to predict the geometry of failure wedge.

- In some research, the failure plane used for analytical model is based on Mohr-Coulomb failure criterion, where:

$$\beta = 45° - \frac{\emptyset}{2} \tag{6}$$

- Merchant proposed that the soil would failure on the path of least resistance. The failure would start from the tip of the tool and reaches to the surface of the soil. The failure angle would be the angle between failure surface and the horizontal. The equation is as followed:

$$\beta = 45^{\circ} + \frac{(90° - \rho) - \emptyset}{2} \tag{7}$$

- Based on the behavior of a rigid plastic material Lee and Shaffer also proposed

a formula for orthogonal cutting problem:

$$\beta = 45^{\circ} + (90° - \rho) - \emptyset \quad (8)$$

FE models also have the capability to predict soil failure angle. In previous studies, equivalent plastic strain field was used in FE models to estimate soil failure angle. [14] [25]

2.4.2 Soil-tool Friction Angle

Friction between two different materials is named external friction. It is an influential parameter in soil cutting process. Unlike soil internal friction, which is considered as an inherent characteristic of the medium, external friction between soil and cutting tool characterizes their interface property. Soil-tool friction is assumed to be constant throughout the soil cutting process. [20] Coulomb friction model was used in many previous reviewed analytical models and numerical models to model friction at the soil-blade interface. The relationship of friction force and friction coefficient is as followed:

$$F_C = \mu F_N \quad (9)$$

It is assumed that sliding between the interfacing surfaces will not happen until the shear stress F_N is the force acting on the interfacing surfaces and μ is the friction coefficient.

2.4.3 Soil Constitutive Models

Both elastic and plastic deformations are observed when soil is under load. Soil response to load is path-dependent. Constitutive laws govern the material's stress-strain behaviour as well as yield criteria with mathematical formulations and thus can describe both the elastic and plastic behaviour of soil. An ideal soil model should be able to predict soil behaviour under all type of loading condition. Formulated constitutive models to describe the behaviour of soils can be categorized as following: linear elastic, non-linear elastic (hyperelasticity, hypoelasticity), variable moduli, elasto-plastic, and elasto-visco-plastic. [26]

Linear elastic stress-strain model is the simplest model to describe stress-strain relation of soil. It is based on the Hook's law. This model is governed by modulus of elasticity and Poisson's ratio. This model is usually inappropriate to be used for highly non-linear behaviour of soils, but in some case piecewise linear elastic models can be used to represent the non-linearity of the problem.

Non-linear elastic model is an extension of the piecewise linear elastic model with infinitesimal linear intervals. Soil constants are assumed to be a function of stress and strain. One of the short coming for this model is that as the direction of strain increment is the same as stress increments in this model, the dilatancy is not considered in this model.

Variable elastic stress-strain law uses different functions to govern the initial loading, unloading and reloading behaviour of soil to reflect the irreversible characteristics of the plastic deformations. Bulk moduli and shear moduli are both considered as non-linear function of the stress and strain tensor invariants.

Elasto-plastic stress-strain models are widely used in governing soil behaviours because they can be defined by few material parameters which can be obtained from standard tests while these models are able to represent important material characteristics of soil such as stress path dependency, dilatancy, and nonlinearity.

Elasto-visco-plasticity theory assumes that plastic strains of soil are time dependent. And unlike elasto-plastic models, elasto-visco-plasticity model assumes that the stress trajectories can cross the yield surface.

When using numerical method to simulate soil material, it is essential to select the appropriate constitutive law. As analysis involves stresses in three directions, most proposed constitutive laws are in three-dimensional space. And as for the need of analysis, they can be simplified to a two-dimensional to solve plane strain problem. The most frequently used constitutive laws in soil mechanics in the past is the Mohr-Coulomb constitutive model. Friction angle and cohesion of soil are used in this model to represent soil strength. Even though this model has the ability to describe the ultimate strength of soil bodies to a satisfactory degree, its possession of corners and apex makes it difficult to use for plastic finite element analysis. For this

reason the Drucker-Prager criterion were proposed by Drucker and Prager [27] and it has been used more and more in recent finite element analysis in place of the Mohr-Coulomb criterion. Drucker-Prager yield function has a conical surface in three-dimension. Its smooth surface makes it simpler to be implanted in the finite element analysis. Modified Cam Clay constitutive law is also used in some research, it is a model based on axisymmetric shear tests experimental of remodeled clay samples. And it is proven to be appropriate to describe the behaviour of soft clays under quasi-static loading condition. [28] For the purpose of this research, Mohr-Coulomb model and Drucker-Prager model are reviewed in details.

Mohr-Coulomb

The Mohr-coulomb model has been widely used to model behaviour of soils. As shown in Figure 5 Mohr Coulomb model is an elastic-perfectly plastic model. With applied load, material firstly deforms linearly according to Hooke's law and when the deformation passes the yield criteria, which is governed by the friction angle (φ) and cohesion (c) of material, material will start to deform plastically. [29]

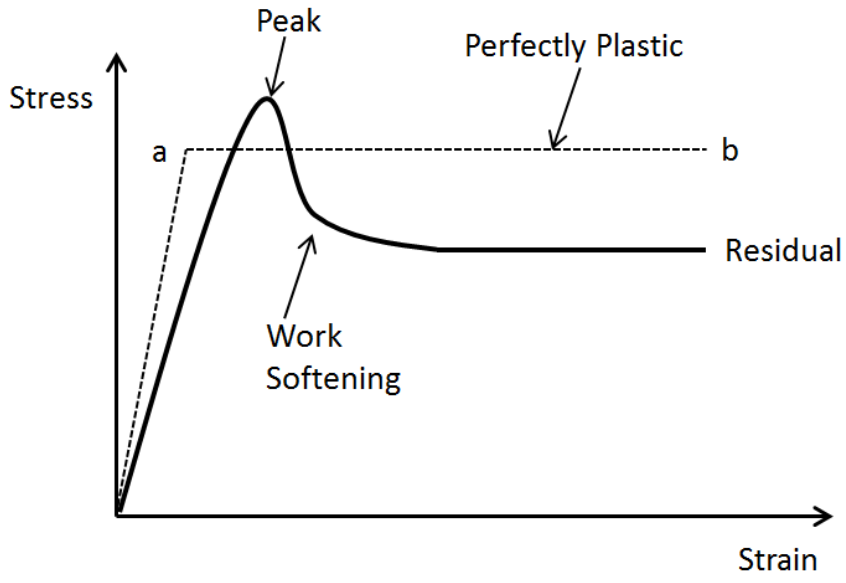

Figure 5 Elastic-perfectly plastic model

The yield surface of Mohr-Coulomb model in principle stress space is a cone shape with a hexagonal cross section and can be expressed by the following expression:

$$\tau = \sigma \tan(\emptyset) + c \tag{10}$$

where τ is the shear strength and σ is the normal stress. $\emptyset$ and c represents the material's internal friction angle and cohesion respectively.

Drucker-Prager

To simulate the elasto-plastic mechanical behavior of soils, Drucker proposed Drucker-Prager yield criterion based on Mohr-Coulomb's yield function in [27]. Drucker-Prager yield criterion simplifies the hexagonal shape of the failure cone to a simpler cone shape. The function of the yield face is written as follow:

$$f = \sqrt{J_{2D}} - \alpha J_1 - k \tag{11}$$

where J_1 is the first invariant of the stress tensor, and J_{2D} is the second invariant of deviatoric stress tensor. α and k represents the positive material parameters that are determined from soil internal friction angle, and are to be calculated from the following equations:

$$\alpha = \frac{2\ sin\emptyset}{\sqrt{3}(3 - sin\emptyset)} \tag{12}$$

$$k = \frac{6c.cos\emptyset}{\sqrt{3}.(3 - sin\emptyset)} \tag{13}$$

2.5 Summary

From the reviews above, it is clear that each approach has its advantages and disadvantages on modeling soil-tool interaction. None of the approach is superior to the others. Which method to use is mainly depends on the nature of the problem under study. Analytical models have clear representation of forces involved and it has the flexibility to include other conditions such as sloped soil surface. However, this approach doesn't help researchers to have a better understanding of the interaction between the blade and surrounding terrains. And because the assumed soil failure shape has significant impact on the model, the accuracy of the simulation lies on the assumed soil failure shape. Empirical models can generate moderately accurate prediction in a very limited condition, but this approach can be very costly and time consuming. It also has limited extensibility and flexibility as the functions are generally not expressed in common parameters of soil. Finite element models have the ability to simulate the reality of earthmoving phenomenon, helps researchers to better understand the soil-tool interaction and the distribution of stress of soil terrain. But it is not suitable for real time implementation due to its computational expense.

Current study intents to use FE model to gain knowledge of soil-tool interaction and then combine this knowledge with analytical method for real-time simulation.

Chapter 3 Material and Finite Element Modeling

In this chapter, the process of finite element modeling to simulate soil cutting phenomenon is outlined. Then the implementations of finite element modeling are explained in details.

3.1 Process of Finite Element Analysis

ANSYS, a commercial finite element software, was used in this research to build and analysis FE model that simulates soil cutting phenomenon. The process of finite element analysis generally involves three stages: pre-processing, analysis, and post-processing.

In the pre-processing stage, the geometry of the model that represents the physical problem is defined and created. This continuum region is discretized into elements by meshing the model. A variety of element shapes are available in the commercial FE software and the selection of the element shape is mainly depends on the application. After the shape of the element is selected, the interpolation function needs to be chosen. Polynomials are usually used as interpolation functions for the field variable. Element properties are then assigned and the matrix equations expressing the behaviour of the entire system are assembled. Boundary conditions are also applied in this stage. [30]

In the solution stage, the output file generated from pre-processing stage is used to construct the element stiffness matrices of each element. And a set of linear or

nonlinear algebraic equations are solved. Type of analysis, load step can also be controlled in this stage before solving the equations.

In the post-processing stage, output file obtained from analysis stage is ready to be used. Complete information of displacements, stresses, and strain are obtained. Depends on the purpose of analysis, different analyzed graphs and tables are available.

3.2 Constitutive Law

In this research, behaviour of soil is considered to be governed by Druker-Prager yield criteria. Non-associate plasticity is applied. As reviewed in Chapter 2, this model is similar to Mohr-coulomb law, but it uses the outer cone approximation. A Drucker-Prager yield model is implemented in ANSYS as a user defined material. [31] To fully defined stress-strain relationship of soil and its flow rule, five parameters are required as input in ANSYS: young's modulus, poisson's ratio, soil cohesion, soil internal friction angle, and soil dilatancy angle. Material properties used are shown in Table 1 Material properties used in current research. One of the advantages of using Drucker-prager yield model is that it uses the same soil parameters as analytical model with addition of two soil properties, elastic modulus and Poisson's ratio, and thus the same soil type can be studied with both methodology at the same time.

Table 1 Material properties used in current research [17] [32]

Properties	Clayey Soil	Sandy loam Soil	Blade
Cohesion (kPa)	47	15.5	
Soil Internal Friction Angle (°)	18.8	31.8	
Dilatancy angle(°)	15	15	
Modulus of Elasticity (kPa)	6870	8067	200,00 0,000
Poisson's ratio	0.35	0.359	0.3
Density (kg/m^3)	1760	1731	

3.3 Description of Finite Element Model

3.3.1 Geometry of Model

To represent soil cutting process, a cutting blade and a soil block are used. Figure 6 illustrates their dimensions. This dimension is selected so that the solution in the vicinity is not affected by the blocks size. The soil block has a height of 0.8m and width of 1.2m. Penetration depth of cutting blade is 0.2m. The operating rake angle varied in the analysis, ranging from 30˚ to 90 ˚.

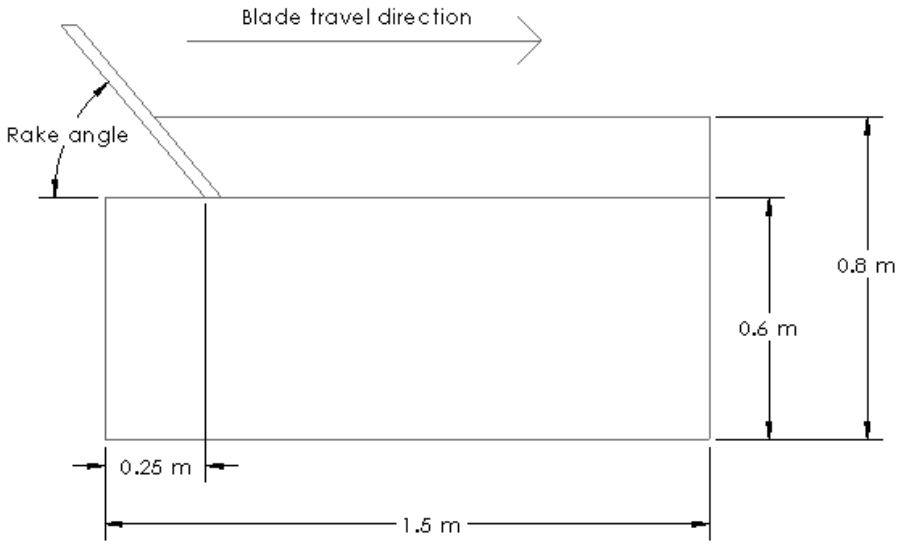

Figure 6 Geometry of FE model

3.3.2 Finite Element Mesh and Boundary Condition

In Ansys software, Plane42 is a 2D 4-noded element with each node has two degrees of freedoms: translation in the nodal X and Y directions. This element has plasticity and strain capabilities and it is used for both blade and soil structures. [33]

Boundary condition is applied to mimic the soil bin testing, and the detail is as follows:

1. Bottom nodes, at Y=0, are fixed in both Y and X direction

2. Nodes on vertical boundaries parallel to Y-axis, at X=0 and X=L are fixed in the X direction.
3. Nodes on blade are fixed in Y direction to limit its displacement in X direction
4. Displacement with small load steps is prescribed for the blade in Y direction

3.3.3 Contact Element

Contact elements are utilized in this research to study the contact stresses transmitted across contacting area. To correctly attach appropriate contact element to the model, the following steps are involved. (1) Identifying contact pairs. (2) Select appropriate contact elements. (3) Designating contact and target surfaces. (4) Select appropriate surface interaction models. (5) Set the real constants and element KEYOPTS for the contact pairs.

The two boundaries that are in contact with each other are the cutting blade and surface of soil that is in contact with the blade. Hence, the contact elements are attached to these two surfaces. A variety of contact element types are available in ANSYS: node-to-node contact, surface-to-surface contact, node-to-surface contact, line-to-line contact, and line-to-surface contact. As surface-to-surface elements are compatible with both lower order and higher order elements, and they support large deformations with significant amounts of sliding and friction efficiently, for the purpose of this research, surface-to-surface contact element is chosen.

After the asymmetric contact pair is identified, it is necessary to designate contact and target surfaces in ANSYS. According to the ANSYS guideline if one surface is stiffer than the other, then the softer surface should be the contact surface and the stiffer surface should be the target surface. So in this soil cutting model contact surface is assigned to the soil and target surface is assigned to the cutting blade. CONTA171 and TARGET 169 were the two contact elements that are suitable for 2-D surface-to-surface contact problems. CONTA171 is a 2-D, 2 node linear element that can be located on the surface of 2-D solid elements. TARGET 169 is the corresponding target element with CONTA171.

During the soil cutting process, soil slides relative to the blade with friction. Five surface interaction models are available in ANSYS. Standard contact also called unilateral contact allows two surfaces to slide with each other with friction and allows opening of the two surfaces when there is no external forces. This contact type is chosen for FE models. [34] Augmented Lagrange formulation is used for contact region. This formulation reduces sensitivity to the contact stiffness and produces less penetration than the pure penalty method.

Chapter 4 Results

4.1 Effect of Mesh Density

As from previous study, the meshing density has significant effect on the predicted force [18], effect of meshing density on the calculated cutting force is studied with model that has rake angle of 50° and smooth tool surface (friction coefficient is zero between soil and blade). Five different meshing densities are used. Identical load steps were prescribed to all five models. For the model with 2306 elements, 3603 elements, 6402 elements and 8636 elements, the edge length of elements were the same for the whole soil block. For the refined model (with 4488 elements), the elements closer to the cutting blade are finer while the other elements are relatively coarser as shown in Figure 7. The obtained cutting force from five models is as shown in Figure 8. The cutting force decreases with the increase in the mesh density. For the model with 6402 elements and the model with 8636 elements, the difference of their calculated cutting force is 1%. The difference between the refined model (4488 elements) and the model with 6402 elements are almost indistinguishable. For the computational efficiency, the model with refined region around the blade is selected to be used for all the rake angles. Elements at the distal region have edge length of 0.025 meter and elements at the refined region have edge length of 0.015 meter.

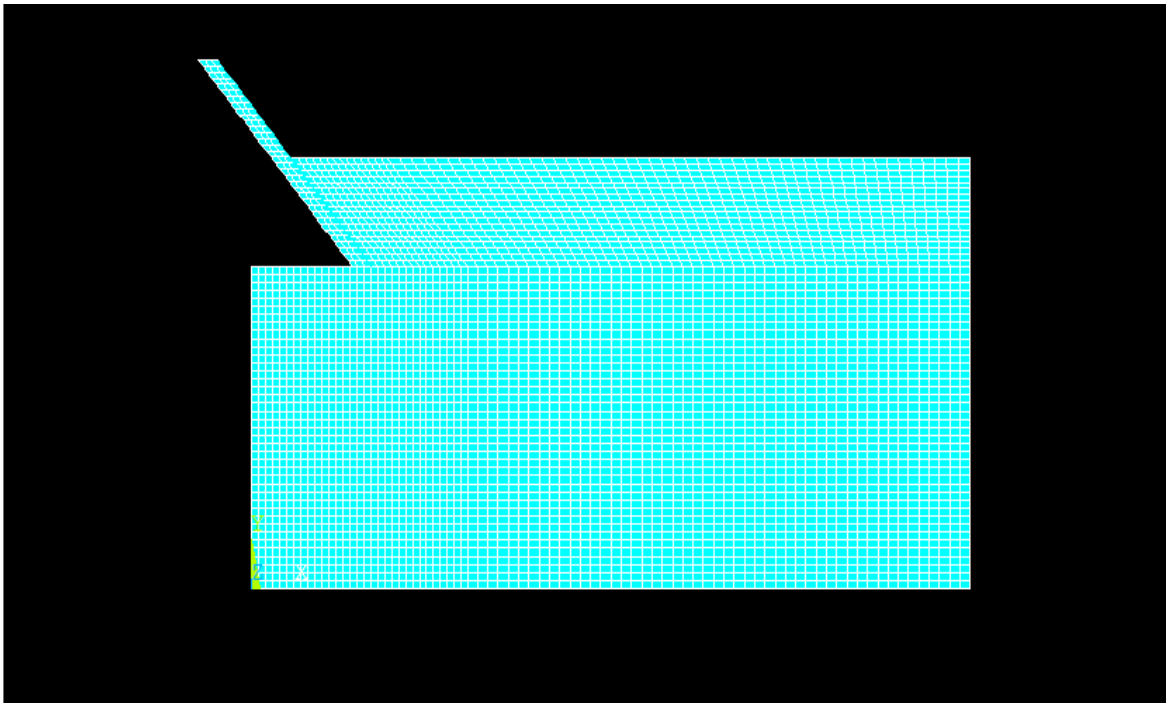

Figure 7 Meshing of FE model

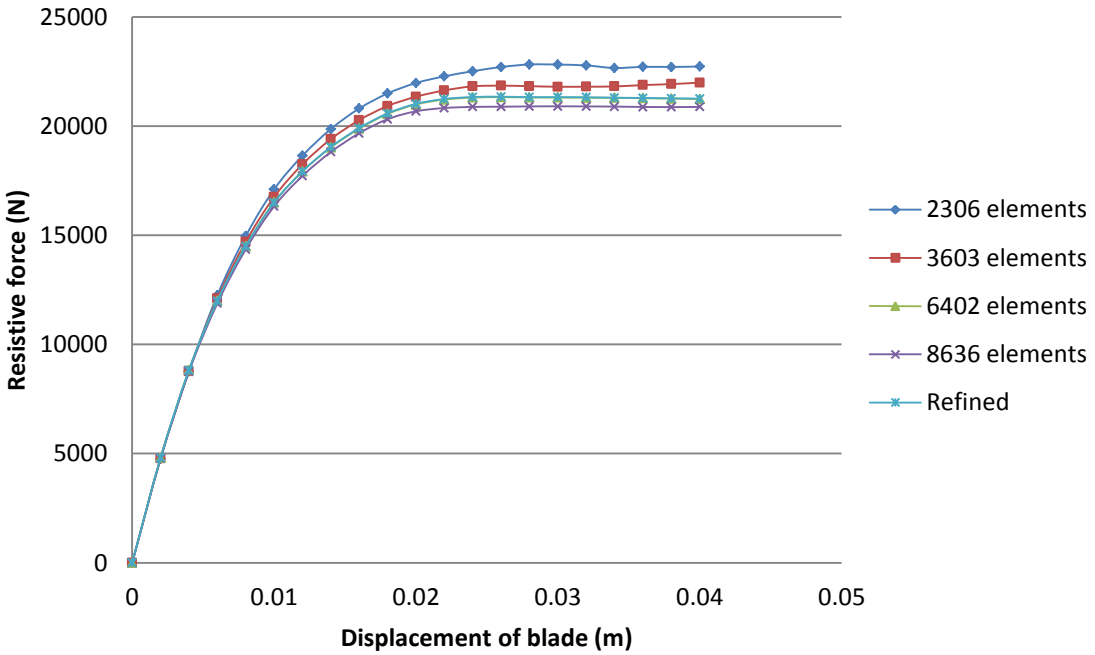

Figure 8 Soil resistive force: rake angle 50°, soil-tool friction coefficient =0

4.2 Soil Failure Angle

Soil failure angle can be obtained by FE model according to the equivalent plastic strain fields. Figure 9 Soil failure angle(a) and (b) shows a failure zone of clayey soil at rake angle of 50˚ and soil-tool friction coefficient of 0.424 and 0 respectively. As reviewed in Chapter 2, three different analytical models are commonly used to predict soil failure angle. In this study, shear angles obtained from FE model are compared with the results obtained from the analytical models.

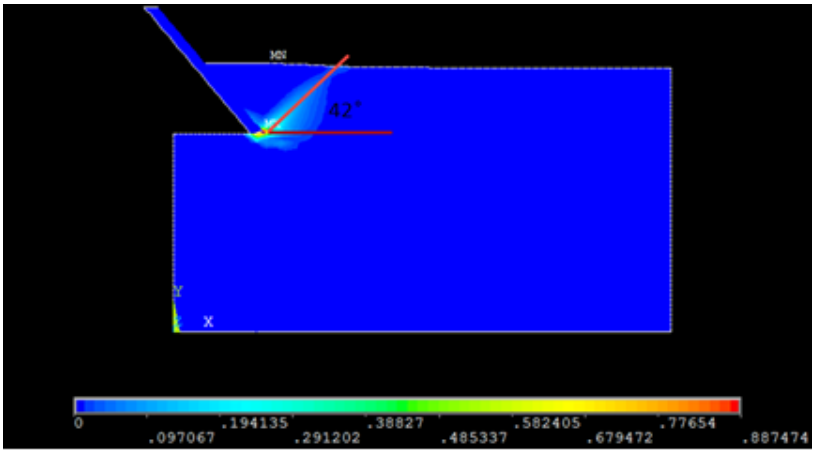

(a)

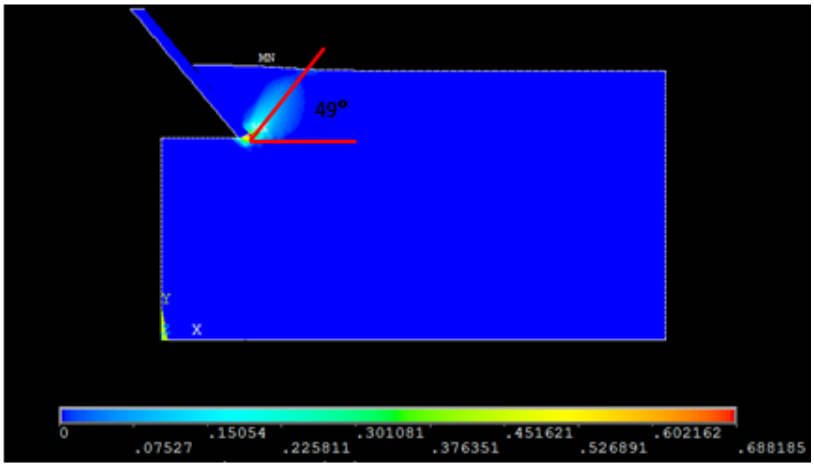

(b)

A

Figure 9 Soil failure angle of clayey soil at rake angle of 50° (a) friction coefficient of 0.424 (b) friction coefficient of 0

Table 2 Predicted soil failure angles of clayey soil by FE model and analytical models and Table 3 listed all the predicted soil failure angles by three different formulas and the measured angles from FE models. It is observed that friction coefficient does have significant effect on the soil failure angle. With the friction coefficient increases from 0 to 0.424, the failure angle for clayey soil decreases by 7° to 13° depends on the rake angle and the failure angle for compacted soil decreases by 8° to 17° depends on the rake angle . This means that with the increase of soil-tool friction coefficient the internal friction contact area will increase which will further lead to the increase of the resultant cutting force.

For smooth blade, results obtained from the FE models have the best accordance with the Merchant model. For clayey soil, the percentage difference of the results ranges from 1.7% to 11.9% for different rake angles. For sandy loam soil, the percentage difference of the results ranges from 4.3% to 15.4%.

Coulomb failure criterion only relate failure angle with soil internal friction angle and thus not change with the increment of rake angle. It under-predicts the failure angle at lower rake angle and is suitable to be used for orthogonal soil cutting.

Lee and Shaffer's model over predicts soil failure angle at lower rake angle up to 26.2° and under predicts soil failure angle at higher rake angle up to 11°. Since the cutting force is directly related to the prediction of soil failure angle, Merchant model is recommended to be used with analytical earth moving equations in future study.

Table 2 Predicted soil failure angles of clayey soil by FE model and analytical models

Clayey soil					
Rake angle	Soil-tool friction coefficient	Soil Failure Angle			
		FE model	Coulomb Failure model	Merchant's failure model	Lee and Shaffer's failure model
30°	0	60°	35.6°	65.6°	86.2°
	0.2	53°			
	0.424	47°			
50°	0	49°	35.6°	55.6°	66.2°
	0.2	47°			
	0.424	42°			
70°	0	42°	35.6°	45.6°	46.2°
	0.2	37°			
	0.424	32°			
90°	0	35°	35.6°	35.6°	26.2°
	0.2	30°			
	0.424	25°			

Table 3 Predicted soil failure angles of sandy loam soil by FE model and analytical models

Sandy loam soil					
Rake angle	Soil-tool friction coefficient	Soil Failure Angle			
		FE model	Coulomb Failure model	Merchant's failure model	Lee and Shaffer's failure model
30°	0	50°	29.1°	59.1°	73.2°
	0.2	46°			
	0.424	42°			
50°	0	47°	29.1°	49.1°	53.2°
	0.2	40°			
	0.424	30°			
70°	0	36°	29.1°	39.1°	33.2°
	0.2	31°			
	0.424	22°			
90°	0	25°	29.1°	29.1°	13.2°
	0.2	17°			
	0.424	12°			

4.3 Blade Cutting Force

4.3.1 Obtaining soil resistive force

In the previous FE model researches; there are two approaches to obtain the force required for soil cutting from the force-displacement curve. One approach is to use the maximum value of the curve as the required force. In other cases, the force-displacement curve kept increasing with the displacement and do not drop down after a number of increments. This is caused by a residual modulus assigned to the failed element. Soil failure zone according to plastic strain intensity used to determine the force in this case. When the failure zone propagates from the tool tip to the soil surface, the corresponding force is chosen to be the required soil force. [15] [25]

As the force-displacement curve for 30˚ rake angle and 50˚ rake angle do not drop down after a number of increments, the second approach is adopted to obtained the soil resistive force. Figure 10 Force-displacement for 50 °rake angle and 0 soil-tool friction coefficientshows the force-displacement curve for model with 50˚ rake angle and soil-tool friction coefficient of 0.424. At displacement of 0.026m, the failure zone propagates from the tool tip to the soil surface, and the corresponding force is selected as the required force to break soil.

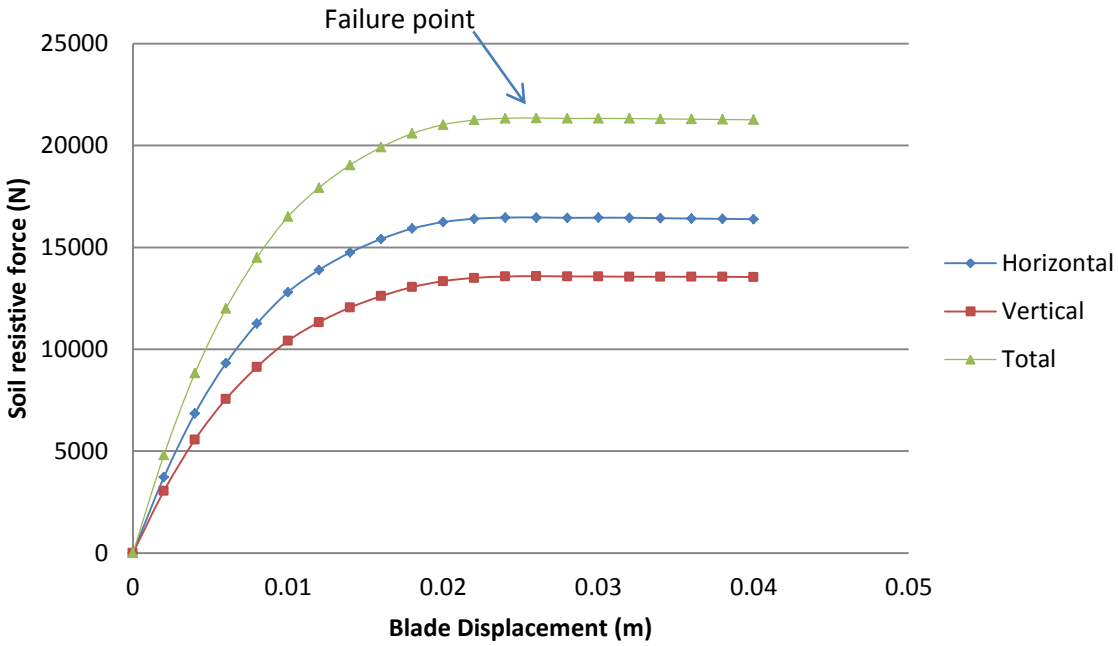

Figure 10 Force-displacement for 50° rake angle and 0 soil-tool friction coefficient.

4.3.2 Effect of rake angle and soil-too friction coefficient

Obtained soil resistance force for each model is shown in Figure 11and Figure 12 Soil resistance force of sandy loam soil. It is observed that with the increase of rake angle the soil resistance increases. It is the case for all three soil-tool friction coefficients. As the rake angle increases the path of the soil plastic strain intensity propagation increases, this may be the major reason for the increase of soil resistance force. For models with 50˚ and 70˚, increment of soil resistive force is getting larger as the friction coefficient increases. For models with90˚ rake angle, the increment firstly increase and then dropped with the increase of friction coefficient.

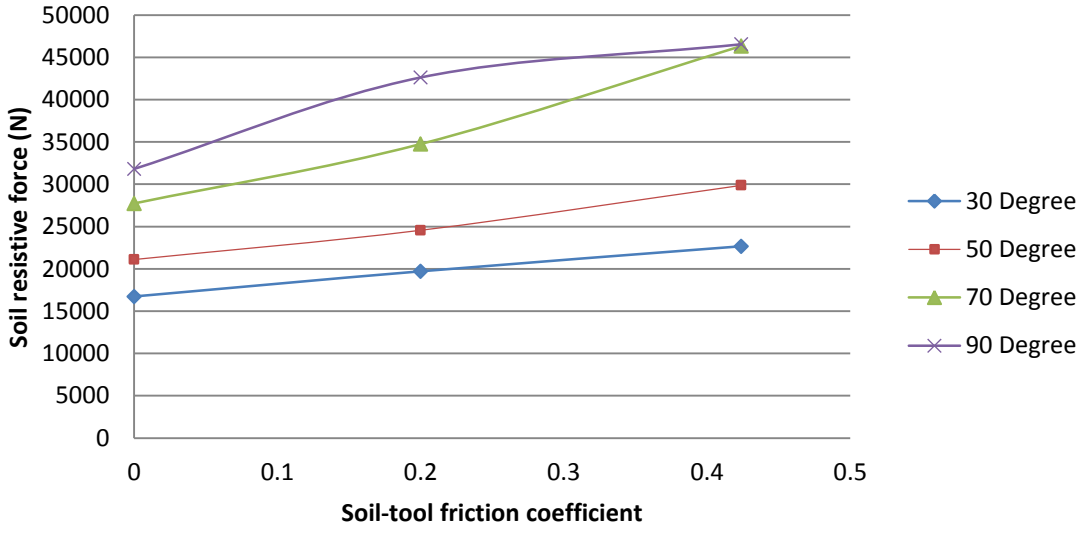

Figure 11 Soil resistive force of clayey soil

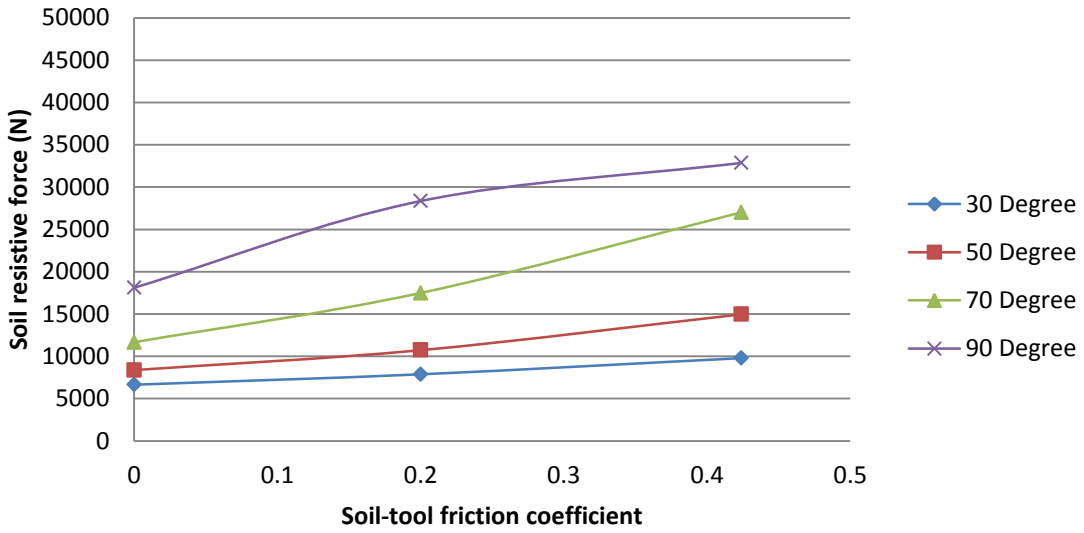

Figure 12 Soil resistance force of sandy loam soil

Obtained results also demonstrate that friction coefficient is directly related to soil resistive force. Predicted resistive force almost increase linearly with respect to friction coefficient. With the increase of rake angle, the increment of resistive force with respect to friction coefficient increases with exception of model with 90˚ rake angle and friction coefficient of 0.424 for both soil type.

Table 4 Soil resistive force of clayey soil

Clayey Soil				
Rake angle	Soil-tool friction coefficient	Fx(N)	Fy(N)	Ftotal(N)
30	0	8560	14378	16733
	0.2	13223	14609	19705
	0.424	18318	13355	22669
50	0	16299	13399	21100
	0.2	21658	11577	24558
	0.424	28629	8503	29865
70	0	26131	9282	27731
	0.2	34386	5008	34749
	0.424	46256	-2728	46336
90	0	31808	-243	31809
	0.2	41830	-8142	42615
	0.424	45183	-11171	46543

Table 5 Soil resistive force of sandy loam soil

Sandy loam soil				
Rake angle	Soil-tool friction coefficient	Fx(N)	Fy(N)	Ftotal(N)
30	0	3123	5861	6641
	0.2	4936	6136	7875
	0.424	7535	6248	9788
50	0	6164	5666	8372
	0.2	9073	5718	10724
	0.424	14089	5037	14962
70	0	10570	4933	11664
	0.2	17191	3196	17486
	0.424	26961	-1759	27018
90	0	18102	-17	18102
	0.2	27816	-5486	28352
	0.424	32227	-6432	32863

Table 4 and Table 5 Soil resistive force of sandy loam soil listed the resistive force for FE model. A comparison of forces obtained from FE model and 2D analytical model is made. Forces obtained from FE model exceed forces obtained from analytical model for all rake angles, soil-tool friction coefficients, and soil types with one exception of model with rake angle 90° and soil-tool friction coefficient of 0.424 of both clayey soil and sandy loam soil. The over-prediction of FE model compared to 2D analytical model ranges from 14% to 35.8% for clayey soil model, and ranges from 29% to 38.4% for sandy loam soil model. This difference is attributed to the following:

- The Drucker-Prager plastic model does not have the ability to account for the crack formation and fragmentation of the soil, which is commonly observed during soil bin test.
- Even though the majority of soil parameters required for analytical model and FE model are the same. There are three soil parameters that are used in FE model but not analytical model. They are Young's modulus of elasticity, Poisson's ratio, and soil dilatancy angle. It is shown in previous study that Poisson's ratio and dilatancy angle do not have significant impact on the prediction of resistive force. However, Young's modulus of elasticity is a factor for prediction of resistive force.
- It is observed from FE model that the predicted failure angle has the best accordance with Merchant's failure model; however with the increase of soil-tool friction coefficient, the soil failure zone also changes. This is not reflected on the analytical model.
- 2D Analytical model is based on the assumption that the soil fail in triangle wedge. The accuracy of resultant force is directly related to the accuracy of the assumed failure wedge shape.

4.4 Force distribution on cutting tool

At the loading step where the soil failure plane fully forms the soil resistive force is obtained. Force distribution on the cutting tool is also studied at this point. Figure 13 Force distribution of model with clayey soil, 0.424 friction coefficient (a) 30° rake angle (b) 50° rake angle (c) 70° rake angle (d) 90° rake angle shows the force distribution for model of clayey soil with soil-tool friction coefficient of 0.424. With the known force distribution, the location of equivalent point force is summarized and the ratio of height of the equivalent point force verses penetration depth in shown in Figure 14 and Figure 15.

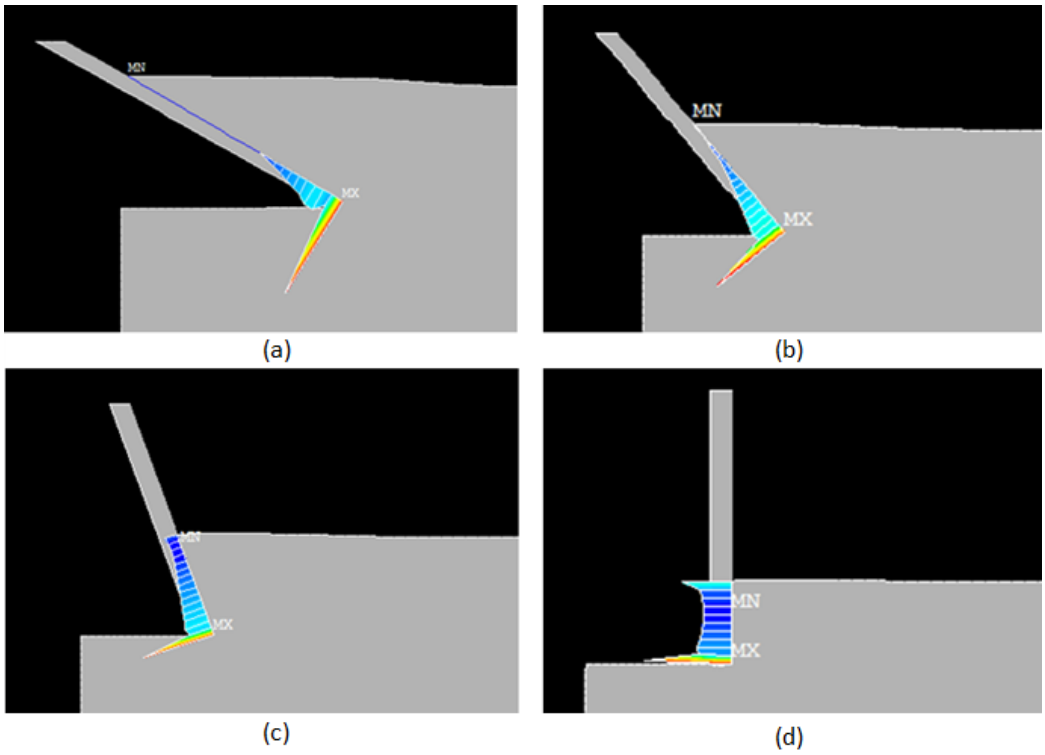

Figure 13 Force distribution of model with clayey soil, 0.424 friction coefficient (a) 30° rake angle (b) 50° rake angle (c) 70° rake angle (d) 90° rake angle

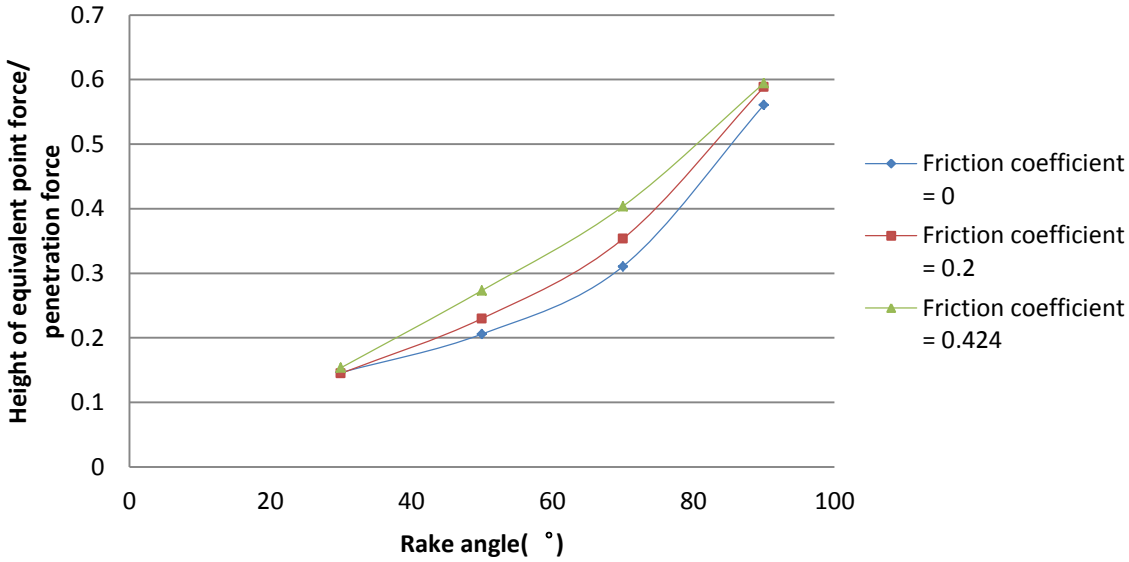

Figure 14 Height of equivalent point force on tool verses penetration depth of clayey soil

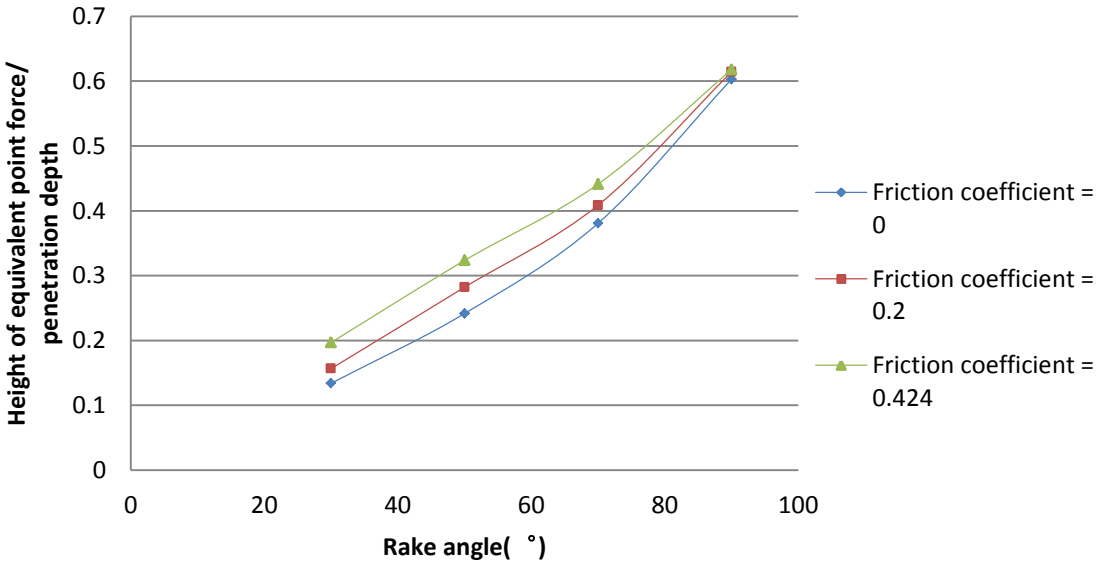

Figure 15 Height of equivalent point force on tool verses penetration depth of sandy loam soil

It is observed that rake angle has significant influence on the location of point force. With the increase of rake angle, the equivalent point force shift from the tip of the cutting tool to a higher location. This is the case for all three friction coefficients

and both soil types. With all the analytical models assume that the point force locates on the tool tip. This research proposes that a moment is added to account for the actual force distribution.

4.5 Validation of FEM

The validity of the model was examined from three aspects: soil failure plane, and soil displacement field.

4.5.1 Soil failure zone

The FE model shows that the soil failure process starts from the tip of the cutting tool and with the increased displacement the failure region extended to the soil surface. The propagation of the soil failure zone is shown in Figure 16. Even though Terzaghi's passive earth press theory assumed that the soil within the failure region is in the state of plastic equilibrium, the field and laboratory experiment indicates otherwise. Chi and Kushwaha observed that the lumps of soil were left on the soil surface after soil cutting. [15] The FE model shows the same phenomena with the lab experiment where not all the soil in front of the blade is failed.

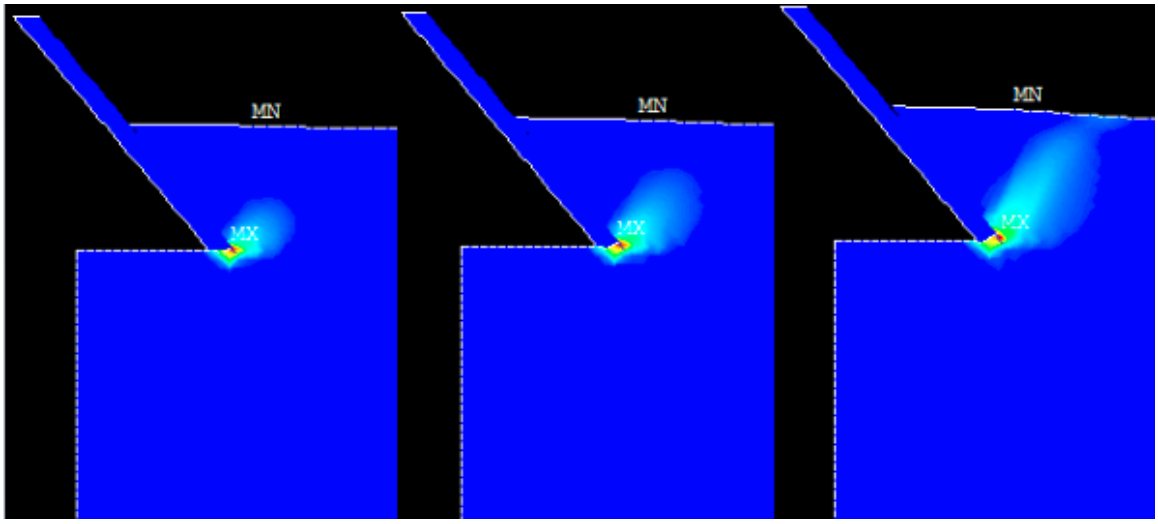

Figure 16 Propagation of soil failure zone from tool tip to soil surface

4.5.2 Soil displacement field

Figure 17 shows the displacement of soil in X-component and Y-component at the load point where the plastic strain intensity propagates to the soil surface. This displacement behaviour agrees with the observation from the field where the failure wedge of soil is pushed forward and upward over the undisturbed soil. [10] [35] In the figure that shows the Y-component displacement, the boundary of the region that has significant displacement would be the separation surface of soil.

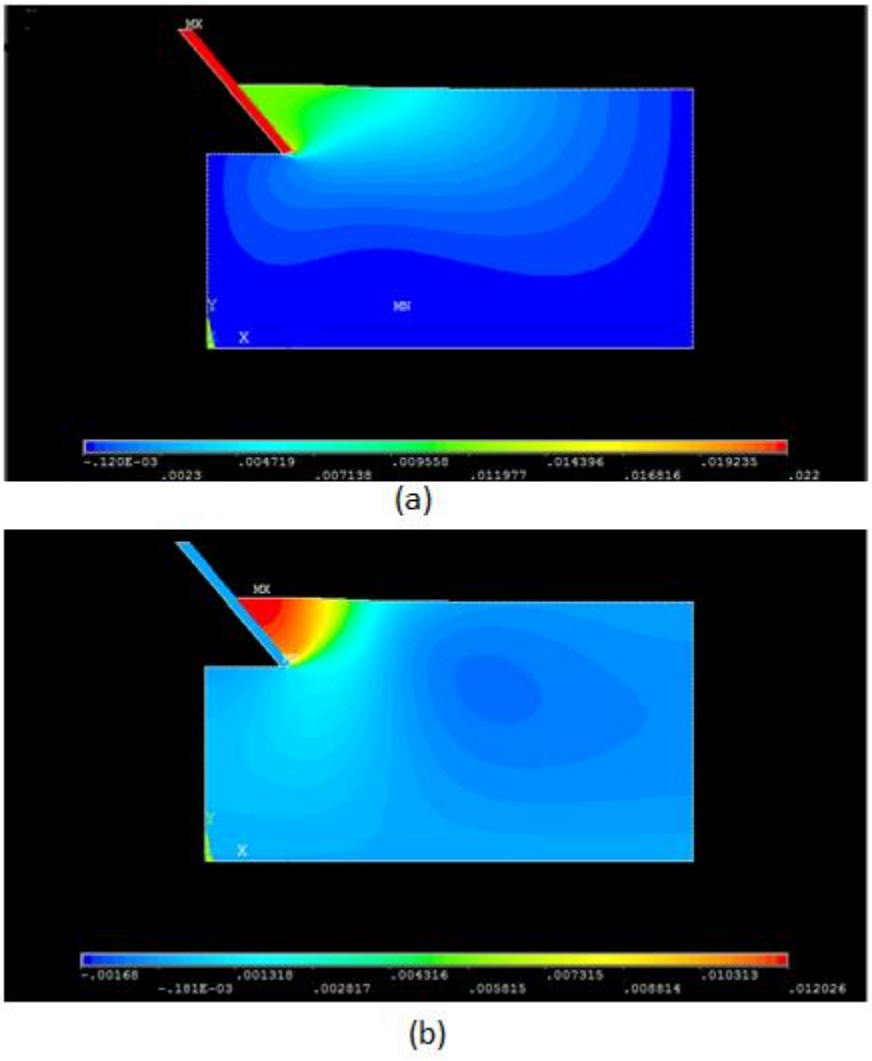

Figure 17 Soil displacement (a) X component; (b) Y component

Chapter 5 Application to Simulating Digging Resistive Force

5.1 Introduction

The intension of this chapter is to demonstrate the procedure to incorporate the knowledge obtained from FE model into the simulation of resistive force during the action of excavation. As results shows that resistive force predicted by FE model and analytical model have a consistent percentage difference, magnitude of resistive force from analytical model is used in this research.

To simulate and predict tool induced soil resistive force the key aspect is to obtain all the required parameters involved in the equations. As explained in chapter 2, parameters that are required can be separated into four distinct groups: tool parameters, soil parameters, soil-tool interface parameters, and surcharge condition.

Soil-tool interface parameter and soil parameters are mainly depends on the soil type and the surface condition of tools. These parameters are usually obtained in lab with experiments. Terrain surcharge condition is determined by the digging environment. All the parameters remains the same throughout the digging process with the given soil type, tool type, terrain condition, and the assumption that the soil is homogeneous. However, tool parameters do vary during the digging process.

5.2 Bucket trajectory

A typical excavator bucket, as shown in Figure 18, consists of a bottom cutting plat, two side plates and a back convex plate. During the digging process, the bottom

plate is acting as the cutting tool that breaks soil and moves the soil from its original place. It provides the force to fail the soil in front of the bucket. Two side plates confines the soil into the bucket and the back convex plate holds the soil that has been broken.

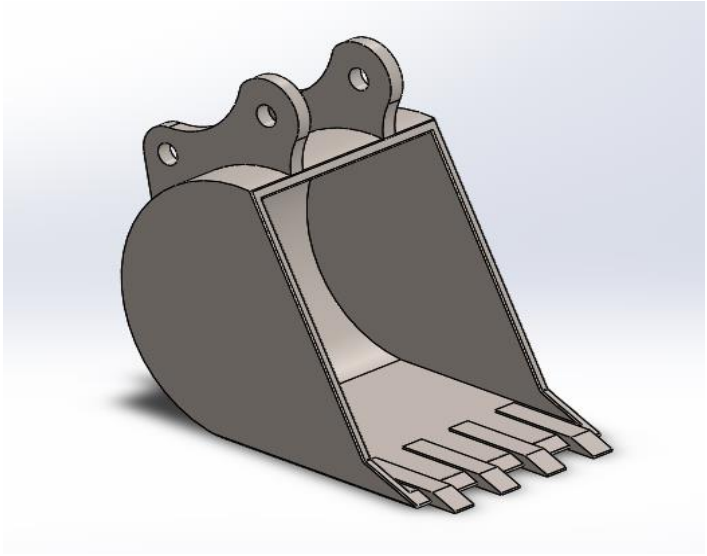

Figure 18 Geometry of excavator bucket

Simulation of interaction force between soil and tool during a typical excavation process requires three tool parameters: width of tool, tool penetration depth, and tool rake angle. Width of tool (w) does not change during the excavation process. It can be simply obtained by measuring the width of bottom plate. Tool penetration depth (d) and tool rake angle (α) varies and they are the two parameters that need to be acquired during the digging cycle. For the case of excavator bucket, tool penetration depth would be the vertical distance between bottom plate edge to the ground and the rake angle would be the angle between bottom plate and the ground.

A bobcat 435 excavator was used by Purdue University to conduct study of multi-actuator displacement controlled mobile hydraulic systems. For the purpose of their study, displacements of hydraulic actuators were recorded during soil digging cycles. Four major linkage components as identified in Figure 19 are connected by hydraulic actuators. And with the manipulation of actuators, to extend them or retract them, the movement of each linkage can be controlled.

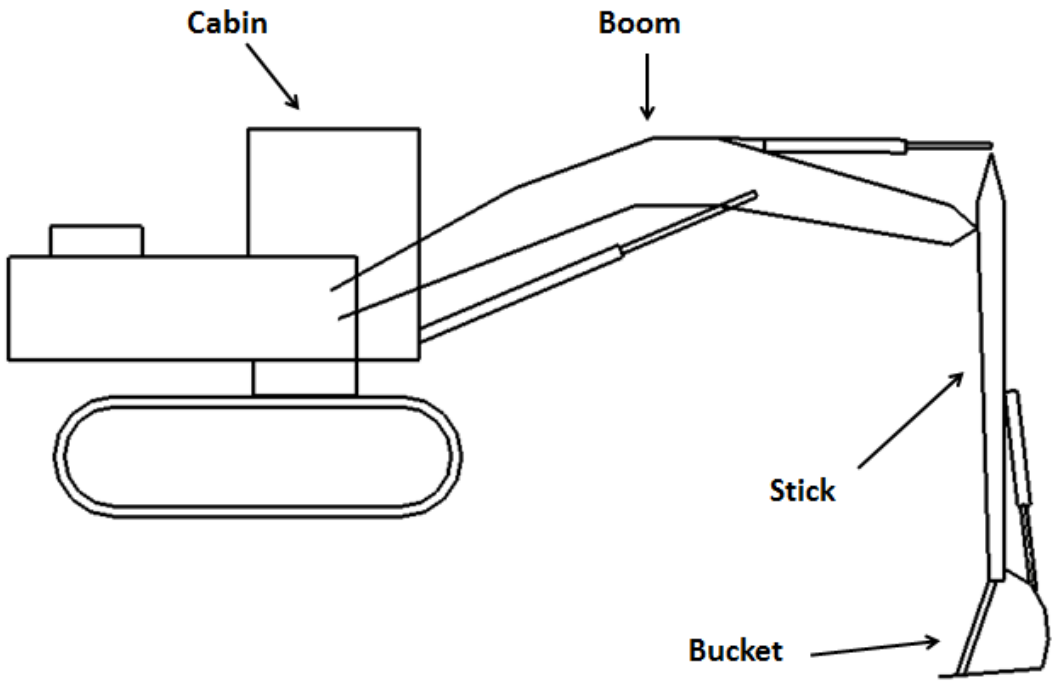

Figure 19 Major link components of excavator

Simmechanics was used in this study to conduct a trajectory study and therefor obtaining the tool parameters. The measurements of length of each linkage and the actuator in its fully retracted position were made. With the kinematic study, bucket trajectory and rake angle is shown in Figure 20 and Figure 21.

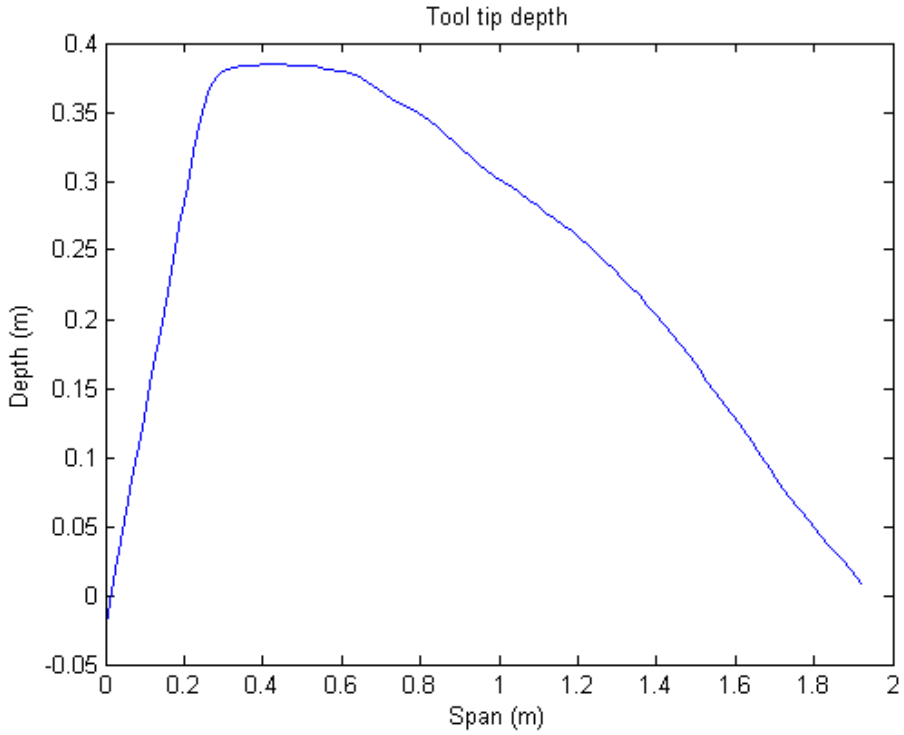

Figure 20 Excavator bucket trajectory

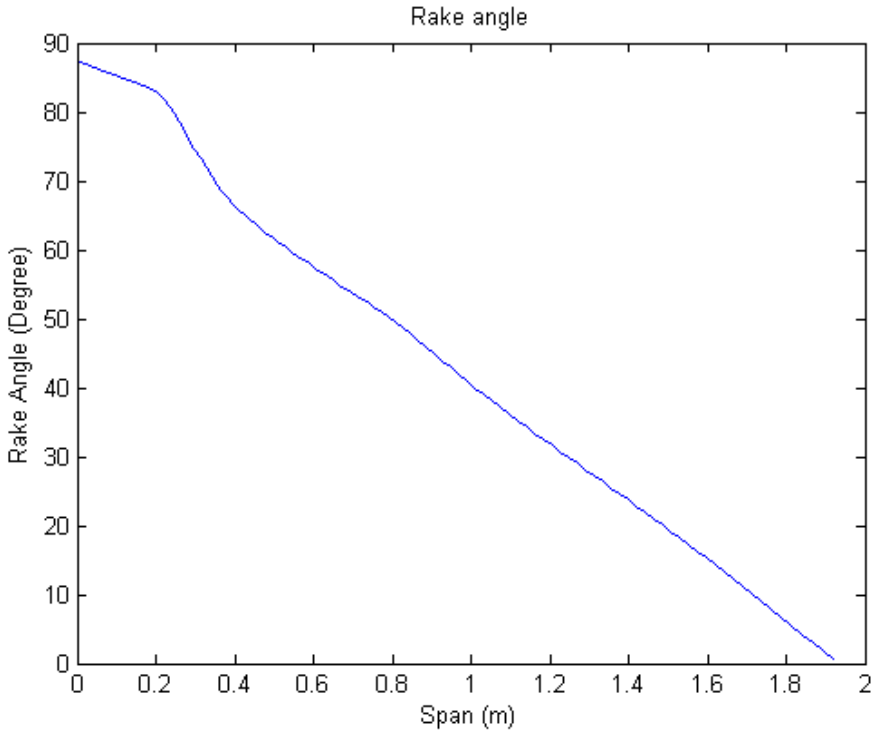

Figure 21 Excavator bucket rake angle

5.3 Simulation of Soil Resistance Force

As the side plates confine soil inside the bucket, this problem can be treated as a two-dimensional plane strain problem. Reece's two-dimensional model is chosen to simulate resistance force for excavator bucket. Instead of using a constant value of soil failure angle, Merchant model is used to predict soil failure for different rake angles. Same soil properties are used in this simulation as used in FE models. The only two parameters that are different is the soil elastic modulus and Poisson's ratio, which is unnecessary for the analytical model. A moment is incorporated in the model to account for the real force distribution on the blade.

Three components of soil resistive force are as shown in Figure 22. The gravity of wedge component has the smallest magnitude while the cohesional force is the major component of the soil cutting force.

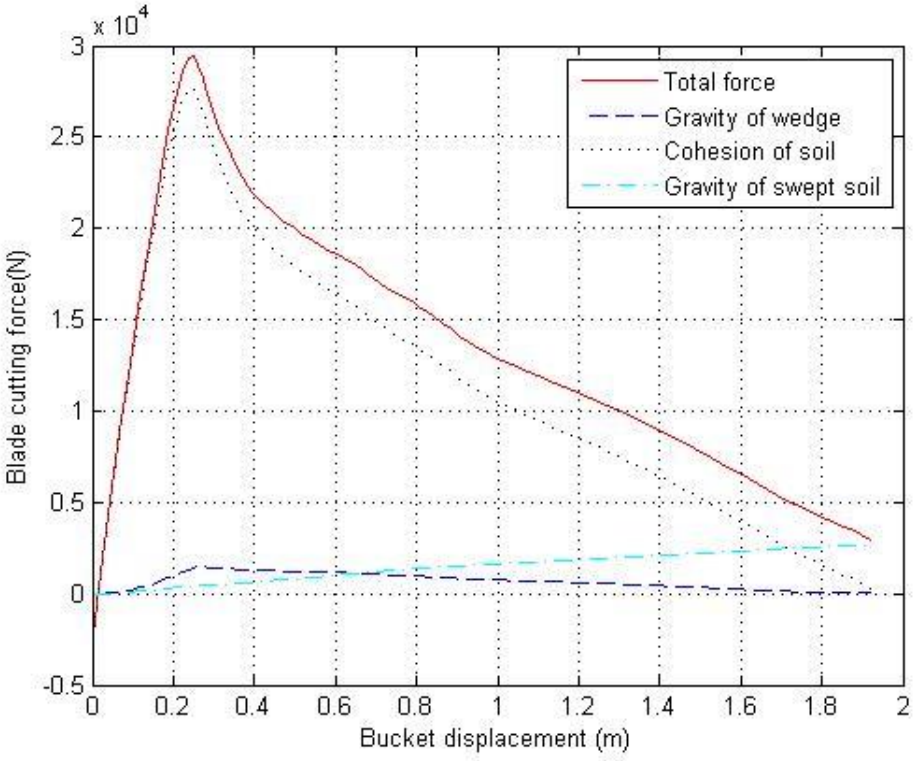

Figure 22 Blade cutting force

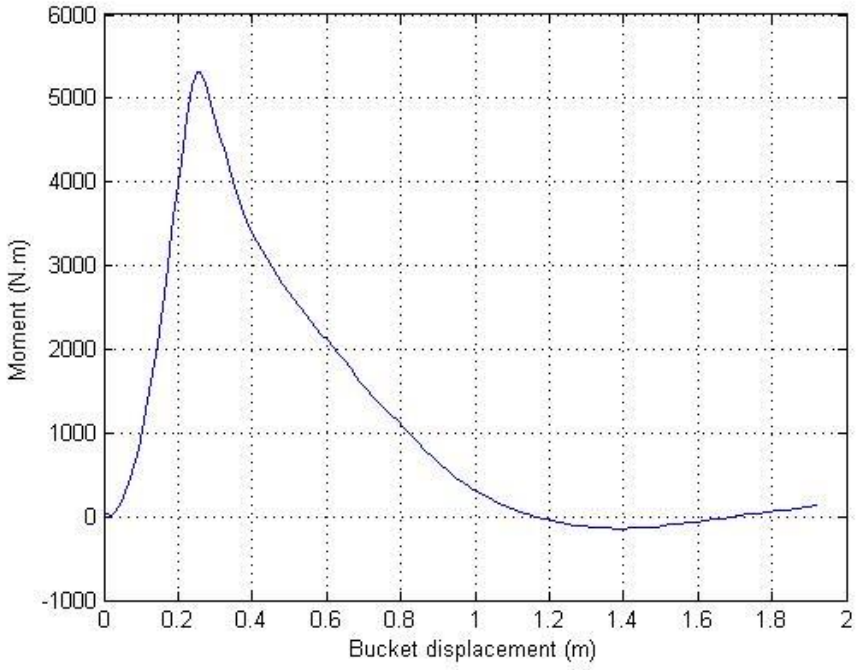

Figure 23 Moment at the blade tip to account for the real stress distribution

Chapter 6 Conclusion and recommendations

6.1 Summary and Conclusions

Even though many FE models have been developed previously, no comprehe sive studies has been conducted to study the effect of soil-tool friction coefficient on soil failure zone, soil resistive force, and stress distribution on the cutting tool. The main objective of this thesis was to attempt to fulfill this need, and utilize the obtained results to improve the simulation of resistive force during excavation process. The findings was helpful in the field of tool design optimization, control system evaluation and excavator simulator.

The research started with literature reviews of analytical models and FE models. Pros and cons of each approach are summarized. FE model was built with different rake angles, friction coefficients and soil types. Soil failure angles were estimated for each model. Blade cutting force was obtained from the blade displacement curve at the loading point where the soil failure zone propagates from the tool tip to the soil surface. Force distributions on the cutting tool were also obtained at the same load step.

In this research, effect of mesh density was studied. It was found that with the increase of mesh density, the predicted cutting force decreases. For the model with 6402 elements and the model with 8636 elements, the difference of their calculated cutting force is 1%. The difference between the refined model with 4488 elements and the model with 6402 elements are almost indistinguishable. For computational

efficiency, the model with refined region around the blade was selected to be used for all the rake angles.

Obtained soil failure planes from FE model were compared with three previously used analytical models. Soil-tool friction coefficient had significant effect on the soil failure plane. With the friction coefficient increased from 0 to 0.424, the failure angle for clayey soil decreased by 7° to 13° and the failure angle for sandy loam soil decreases by 8° to 17° for different rake angles. It was found that soil failure plane changes with rake angle as well as soil-tool friction coefficient. The obtained failure angle for smooth blade (soil-tool friction coefficient is 0) has the best accordance with Merchant's model. Coulomb failure criterion only related failure angle with soil internal friction angle and thus not change with the increment of rake angle. It under-predicts the failure angle at lower rake angle and is suitable to be used for orthogonal soil cutting. Lee and Shaffer's model over-predicts soil failure angle at lower rake angle up to 26.2° and it under predicts soil failure angle at higher rake angle up to 11°.

Locations of equivalent point force on cutting tool for different cutting angles were established in this research. Rake angle had significant influence on the location of point force. With the increase of rake angle, the equivalent point force shift from the tip of the cutting tool to a higher location. Soil-tool friction coefficient also has small influence. As all the analytical model assumes that the location of cutting force is at the tip of the cutting tool. It was also proposed in this research to add a moment component to the analytical model to account for the real stress distribution.

The process of obtaining resistive force during a typical excavation procedure was demonstrated. A moment was added to the simulation based on the findings from FE model.

6.2 Recommendations for future work

With the progress made from current research, some suggestions to improve future studies are listed as following:

- Only one penetration depth was studied in this research. Parametric study should be conducted with different blade cutting depths.
- The validation of this research is through previous observed phenomena during soil cutting procedure; lab experiment would be helpful to further compare the magnitude of the predicted soil cutting force.

References

[1] S. P. DiMaio, S. E. Salcudean, C. Reboulet, S. Tafazoli and K. Hashtrudi-Zaad, "A virtual excavator for controller development and evaluation," in *IEEE International Conference on Robotics and Automation*, Leuven, 1998.

[2] F. Malaguti, "Soil machine interaction in digging and earthmoving automation," in *Proceeding of the 11th International Symposium on Automation and Robotics in Construction*, 1994.

[3] O. Luengo, "Modeling and identification of soil-tool interaction in automated excavation," in *IEEE/RSJ International Conference on Intelligent Robots and Systems*, Victoria, 1998.

[4] S. Ashrafizadeh, "Soil failure model in front of a tillage tool action-a review," in *CSAE*, Montreal, 2003.

[5] W. Hong, "Modeling, estimation, and control of robot-soil interactions," MA, 2001.

[6] E. McKyes, Soil Cutting and Tillage, Elsevier, 1985.

[7] R. L. Kushwaha, L. CHI and J. Shen, "Analytical and numerical models for predicting soil forces on narrow tillage tools - a review," *Canadian Agricultural Engineering,* vol. 35, no. 3, pp. 183-193, 1993.

[8] S. Singh, "Learning to predict resistive forces during robotic excavation," in *IEEE International Conference on Robotics & Automation*, Nagoya, 1995.

[9] A. R. Reece, "The fundamental equation of earthmoving mechanics," in *Proceeding of the Institution of Mechanical Engineers*, 1964.

[10] P. C. J. Payne, "The relationship between the Mechanical Properties of soil and the performance of simple cultivation implements," *Journal of Agricultural Engineering Research,* vol. 1, no. 1, pp. 23-50, 1956.

[11] D. R. P. Hettiaratchi and A. R. Reece, "Symmetrical three-

dimensional soil failure," *Journal of Terramechanics,* vol. 4, no. 3, pp. 45-67, 1967.

[12] R. Godwin and G. Spoor, "Soil failure with narrow tines," *Journal of Agricultural Engineering Research,* vol. 22, no. 3, pp. 213-228, 1977.

[13] E. McKyes and O. Ali, "The cutting of soil by a narrow blade," *Journal of Terramechanics,* vol. 14, no. 2, pp. 43-58, 1977.

[14] R. N. Hanna and A. W. Yong, "Finite element analysis of plane soil cutting," *Journal of Terramechanics,* vol. 14, no. 3, pp. 103-125, 1977.

[15] L. Chi and R. L. Kushwaha., "A non-linear 3D finite element analysis of soil failure with tillage tools," *Journal of Terramechanics,* vol. 27, no. 4, pp. 343-366, 1990.

[16] J. Shen and R. L. Kushwaha, "Investigation of an algorithm for non-linear and dynamic problems in soil-machine systems," *Computers and Electronics in Agriculture,* vol. 13, no. 1, pp. 51-66, 1995.

[17] A. M. Mouazen and M. Nemenyi, "Finite element analysis of subsoiler cutting in nonhomogeneous sandy loam soil," *Soil and Tillage Research,* vol. 51, no. 1-2, pp. 1-15, 1999.

[18] M. Abo-elnor, R. Hamilton and J. Boyle, "Simulation of soil-blade interaction for sandy soil using advanced 3D finite element analysis," *Soil and Tillage Research,* vol. 75, no. 1, pp. 61-73, 2004.

[19] U. A. Rosa and D. Wulfsohn, "Constitutive model for high speed tillage using narrow tools," *Journal of Terramechanics,* vol. 36, no. 4, pp. 221-234, 1999.

[20] M. G. Lipsett and R. Y. Moghaddam, "Modeling Excavator-Soil Interaction," in *Bifurcations, Instabilities and Degradations in Geomaterials*, Springer Berlin Heidelberg, 2011, pp. 347-366.

[21] R. H. Karol, Chemical grouting and soil stabilization, revised and expanded, CRC Press, 2003.

[22] B. G. Look, Handbook of Geotechnical Investigation and Design Tables, 2nd ed., CRC Press, 2014, pp. 85-99.

[23] B. Das, Principles of Geotechnical Engineering, 2009.

[24] J. C. Santamarina and H. Shin, "Friction in granular media," in *Meso-Scale Shear Physics in Earthquake and Landslide mechanics*, CRC Press, 2009, pp. 159-190.

[25] O. Pantalé, J.-L. Bacaria, O. Dalverny, R. Rakotomalala and S. Caperaa, "2D and 3D numerical models of metal cutting with

damage effects," *Computer Methods in Applied Mechanics and Engineering,* vol. 193, no. 39-41, pp. 4383-4399, 2004.

[26] H. Kempfert and B. Gebreselassie, "Constitutive soil models and soil parameters," in *Excavations and Foundations in Soft Soils*, Springer Berlin Heidelberg, 2006, pp. 57-116.

[27] D. C. Drucker and W. Prager, "Soil mechanics and plastic analysis for limit design," *Quarterly of Applied Mathematics,* pp. 157-165, 1952.

[28] O. Brown, "Finite element analysis of blade-formation interactions in excavation," 2012.

[29] R. R. Sandhay, P. K. Nagendra and K. T. Sai, "Applicability of Mohr-Coulomb & Drucker-Prager models for assessment of undrained shear behaviour of clayey soils," *International Journal of Civil Engineering and Technology,* vol. 5, no. 10, pp. 104-123, 2014.

[30] K. H. Huebner, The finite element method for engineers, Wiley, 2012.

[31] "Ansys Mechanical APDL Theory Reference. Version 15," 2013. [Online]. Available: http://148.204.81.206/Ansys/readme.html. [Accessed 2016].

[32] X. H. Zhu and Y. J. Jia, "3D mechanical modeling of soil orthogonal cutting under a single reamer cutter based on Drucker-prager criterion," *Tunnelling and Underground Space Technology,* vol. 41, pp. 255-262, 2014.

[33] "Ansys Mechanical APDL Element Reference," 2013. [Online]. Available: http://148.204.81.206/Ansys/readme.html. [Accessed 2016].

[34] "Ansys Mechanical APDL Contact Technology Guide. Version 15," 2013. [Online]. Available: http://148.204.81.206/Ansys/readme.html. [Accessed 2016].

[35] J. C. Siemens, J. A. Weber and T. H. Thornburn, "Mechanics of soil as influenced by model tillage tools," *Transactions of the ASAE,* vol. 8, no. 1, pp. 1-7, 1965.